Band Fluorescence Spectra in Mercury 6($^3P_1$) Photosensitization

O. P. Strausz,* J. M. Campbell, S. De Paoli, H. S. Sandhu, and H. E. Gunning

Contribution from the Department of Chemistry, University of Alberta, Edmonton, Canada. *Received May 12, 1972*

Abstract: Medium high resolution band fluorescence spectra have been photographed in the room-temperature Hg 6($^3P_1$) photosensitization of the noble gases, paraffins, fluoromethanes, ammonia, water, ethanol, ethers, N_2, and CO. In addition to structural details previously unresolved, new band systems on both sides of the 2537-Å resonance line were detected. Bands on either side, but close to the resonance line, originate from loosely bound, quantized van der Waals molecules formed between the excited mercury atom and the substrate. Using Mulliken's recently developed theory, Lennard-Jones force constants were computed from the observed shifts of the satellite bands for the interaction of the excited mercury atom with the various substrates investigated. Ramifications of the spectroscopic observation with regard to the energy transfer step in mercury photosensitization are discussed.

The effect of foreign gases on the spectra of metal vapors has been studied extensively during the past several decades.[1,2] The majority of studies has been directed toward the experimental and theoretical investigation of pressure broadening and associated phenomena, namely the appearance of the so-called satellite bands in absorption spectra. These diffuse bands may appear on either or both sides of the atomic resonance line and their number and position depend on the nature of the metal atom and perturbing gas as well as on the experimental conditions employed.

Satellite bands have also been observed in fluorescence. Oldenberg[3] first reported such bands in the fluorescence spectra of mercury–noble gas mixtures excited by the 2537-Å mercury resonance line. In the presence of neon only one band appeared on the short wavelength side of the resonance line, while Ar, Kr, and Xe each gave more than one diffuse band. In addition, Oldenberg also noted discrete band structures on the long wavelength side of the resonance line when Ar or Kr was present. Kuhn and Oldenberg[4] interpreted these bands as being due to transitions originating from loosely bound excited molecules of the excited metal atom and perturber gas atom. Later, Preston[5] studied the emission spectra of mercury with low pressures of noble gases in a discharge tube and measured the intensities of the satellites relative to the resonance line.

In 1934 Glockler and Martin[6] reported red-shifted emission bands from mercury–methane mixtures and assigned them to transitions from the [Hg 6($^3P_1$)–CH_4] complex.

Besides their inherent interest these band spectra are of paramount importance with regard to the microscopic details of energy transfer processes involving metal atoms. Regrettably the relevance of these early literature reports on the satellite band emission phenomena to the energy transfer step have been completely overlooked by photochemists for over three decades.

The appearance of band fluorescence from irradiated mixtures of mercury vapor with a variety of quenchers including paraffins, water, ammonia, the noble gases, etc., was reported from this laboratory[7] in 1966. The spectra were of rather poor quality owing to the crude optical instrumentation used but appeared to lie in the vicinity of the 2537-Å mercury line. The appearance of band fluorescence was characteristic for low and medium efficiency quenchers; highly efficient ones such as hydrogen and olefins did not show emission. In a subsequent communication[8] it was proposed that the quenching of the 2537-Å radiation of mercury by the noble gases is due entirely to band fluorescence rather than to a "collision of the first kind" *via* potential energy curve crossing as had been considered before.

In more recent developments Freeman, McEwan, Claridge, and Phillips[9-15] have reported in a continuing series of papers since 1970 good quality medium resolution fluorescence spectra of the mercury–ammonia, amines, water, alcohols, and xenon systems. These authors attributed the single, structureless fluorescence bands observed in each case, to transitions from a "charge transfer" complex formed between an Hg 6($^3P_0$) atom and a substrate molecule.

The nature and precise origin of satellite bands in atomic spectra are not well understood and several widely different and sometimes conflicting explanations have been offered.[16-25] One of these attributes the

(1) A. C. G. Mitchell and M. W. Zemansky, "Resonance Radiation and Excited Atoms," Macmillan, New York, N. Y., 1934, p 87.
(2) P. Pringsheim, "Fluorescence and Phosphorescence," Interscience, New York, N. Y., 1949, p 224.
(3) O. Oldenberg, *Z. Phys.*, **47**, 184 (1928); **49**, 609 (1928); 50, 580 (1928); **51**, 40, 605 (1928); **55**, 1 (1929).
(4) H. Kuhn and O. Oldenberg, *Phys. Rev.*, **41**, 72 (1932).
(5) W. M. Preston, *ibid.*, **51**, 298 (1937).
(6) G. Glockler and F. W. Martin, *J. Chem. Phys.*, **2**, 46 (1934).
(7) S. Penzes, O. P. Strausz, and H. E. Gunning, *ibid.*, **45**, 2322 (1966).
(8) H. E. Gunning, S. Penzes, H. S. Sandhu, and O. P. Strausz, *J. Amer. Chem. Soc.*, **91**, 7684 (1969).
(9) R. H. Newman, C. G. Freeman, M. J. McEwan, R. F. C. Claridge, and L. F. Phillips, *Trans. Faraday Soc.*, **66**, 2827 (1970).
(10) C. G. Freeman, M. J. McEwan, R. F. C. Claridge, and L. F., Phillips, *Chem. Phys. Lett.*, **8**, 266 (1971).
(11) C. G. Freeman, M. J. McEwan, R. F. C. Claridge, and L. F. Phillips, *ibid.*, **9**, 578 (1971).
(12) C. G. Freeman, M. J. McEwan, R. F. C. Claridge, and L. F. Phillips, *Trans. Faraday Soc.*, **66**, 2974 (1970); **67**, 2004 (1971).
(13) C. G. Freeman, M. J. McEwan, R. F. C. Claridge, and L. F. Phillips, *ibid.*, **67**, 67 (1971).
(14) R. H. Newman, C. G. Freeman, M. J. McEwan, R. F. C. Claridge, and L. F. Phillips, *ibid.*, **67**, 1360 (1971).
(15) C. G. Freeman, M. J. McEwan, R. F. C. Claridge, and L. F. Phillips, *Chem. Phys. Lett.*, **6**, 482 (1970).
(16) S. Ch'en and M. Takeo, *Rev. Mod. Phys.*, **29**, 20 1957).
(17) A. Michels, H. de Kluiver, and C. A. Ten Saldam, *Physica (Utrecht)*, **25**, 1321 (1959).
(18) L. Klein and H. Margenau, *J. Chem. Phys.*, **30**, 1556 (1959).
(19) O. Jefmenko, *ibid.*, **37**, 2125 (1962); **42**, 205 (1965).
(20) J. Szudy, *Acta Phys. Pol.*, **A38**, 779 (1970); *Bull. Acad. Pol. Sci., Ser. Sci., Math., Astron. Phys.*, **17**, 315 (1969); S. Chudrynski and T. Grycuk, *ibid.*, 13, 693 (1965); J. Fiutak and M. Frackowiak, *ibid.*, 11, 175 (1963).

bands to the existence of vibrational[17,18,24] or quantized vibrational–rotational[20] states of the van der Waals molecules formed between the radiating atom and the foreign gas molecules. Red satellite bands have also been interpreted in terms of the quasistatic theory of pressure broadening of spectral lines.[21,22] Another theory attempts to account for the bands in terms of potential curve profiles without invoking the existence of vibrational states.[19] It has also been suggested that the satellites may also arise *via* a phenomenon which is the precise analog of predissociation of stable molecules.[25]

In a recent article[26] Mulliken discussed the role of kinetic energy in Franck–Condon transitions. Contrary to earlier views he has shown for some model diatomic cases that, in transitions to or from a bound state with sufficient vibrational energy, an additional strong maximum can occur in the transition probability–frequency function particularly if the two electronic potential curves differ significantly. Classically this corresponds to internuclear distances where the nuclei in the initial state have maximum kinetic energy. Mulliken[27] has explained the occurrence of the diffuse bands around $\lambda \sim 3250$ Å in the emission spectrum of the iodine molecule in terms of this theory.

In recent years we photographed a set of full spectra under medium high resolution which probably represents the most extensive compilation of spectral data on mercury band fluorescence. It is the purpose of this article to report these results along with the Lennard-Jones force constants computed from the spectra with the aid of Mulliken's theory.

Experimental Section

High-vacuum techniques were employed throughout. The fluorescence cell consisted of a 10 × 120 mm Spectrosil tube with plane 1/8-in. thick LiF windows. The outlet and inlet tubes were sealed close to the windows to ensure complete circulation of the gas. In some experiments the above cell was replaced by a 10 × 200 mm double wall Spectrosil cell which allowed the use of a filter solution of 6-mm radial path length surrounding the reaction cell. This solution consisted of a 1:1 aqueous mixture of concentrated $NiSO_4$–$CoSO_4$ solution and an "ultraviolet dye"[28] and had a transmission of about 1% at 4047 Å and about 3% at 2967 and 4358 Å compared to that at 2537 Å. Closely spaced, blackened brass plates collimated the exciting light beam. A Hanovia low-pressure mercury lamp, No. 87a-45, placed parallel to the emission cell, was the radiation source. A stream of nitrogen cooled the lamp slightly and prevented ozone formation within the cell enclosure.

The light emerging from the end of the cell was focused onto the entrance slit (normally 20 μm) of a Hilger-Watts medium quartz spectrograph. Kodak 103a-0 photographic plates with a linear response from 2400 to 5000 Å were used throughout. The plates were developed in Kodak D-19 developer for 3.5–5 min (25°) and microdensitometry was carried out on a Joyce, Lobel automatic recording MKIIIC instrument. The photographic plates were preexposed for 15 sec to weak white light prior to the experiment to ensure that the optical density of the plate was linear with the logarithm of light intensity.

In a typical run a ballast pressure was first established by a low temperature bath. The flow and pressure of the gas in the cell were controlled by two Edward needle valves and measured on a Matheson R-2-15AAA rotameter. The mercury saturator was maintained at 20°. Exposure times varied from 30 sec to 5 hr depending on the intensity.

The materials used were of the highest purity available. If necessary, compounds were purified until no impurities were detectable with vapor phase chromatography.

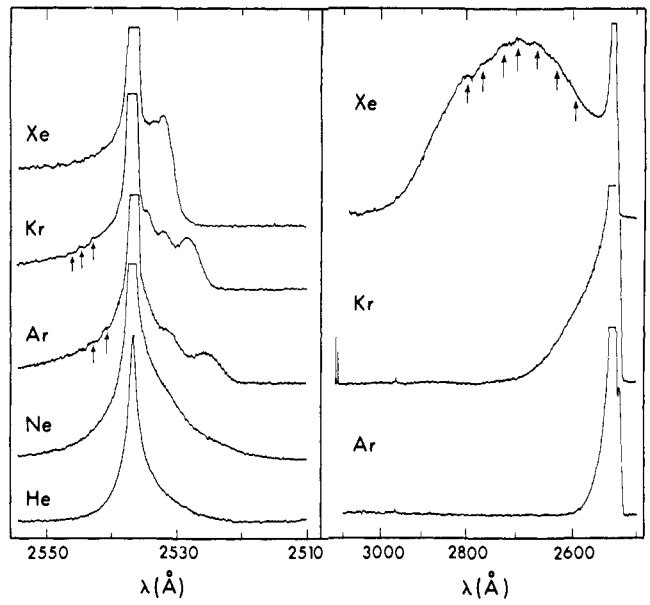

Figure 1. Microdensitometer trace of emission spectra for various noble gases. Maximum deflection for each curve is 2.16 optical density units (OD) unless specified otherwise. Left: He, 430 Torr, 4.5 hr; Ne, 440 Torr, 1.5 hr; Ar, 600 Torr, 21 min; Kr, 750 Torr, 10 min; Xe, 860 Torr, 30 min. Right: Ar, 400 Torr, 33 min (0.8 OD); Kr, 750 Torr, 30 min (0.8 OD); Xe, 830 Torr, 10 min (0.8 OD); faint structures in spectra are marked with arrows.

Results

The fluorescence spectra are reproduced in Figures 1 to 6, and the separation of the band maxima from the resonance line is summarized in Tables I and II. According to their location the bands can be divided into three distinct types. The type "a" bands appear at a few ångströms (±20 Å) on either side of the 2537-Å

Table I. Separation of Emission-Band Maxima (cm^{-1}) from the 2536.5-Å (39,424 cm^{-1}) Resonance Line

Compd	Pressure, Torr	a bands $\Delta\omega_1$	a bands $\Delta\omega_2$	a bands $\Delta\omega_3$	b bands $\Delta\omega$
Ar	400	~27	77	164	
Kr	180	~30	70	128	
Kr	750	~30	74	128	
Xe	10		58		−1830
Xe	860	~36	58		−2380
CH_4	220	65			
C_2H_6	330	29			
C_3H_8	600				−1260
i-C_4H_{10}	645				−1260
$C(CH_3)_4$	8				−1560
$C(CH_3)_4$	510				−1830
c-C_3H_6	400				−2250
c-$C_3H_4(CH_3)_2$	80				−1550
c-C_5H_{10}	210				−1400
c-C_6H_{12}	72				−1770
CH_3F	330				−1500
CHF_3	280	−97			
CF_4	614	220			
SF_6	190	220			

(21) J. Kieffer, *J. Chem. Phys.*, 51, 1852 (1969).
(22) J. M. Farr and W. R. Hindmarsh, *Phys. Lett. A*, 27, 512 (1968).
(23) J. F. Kielkopf, J. F. Davis, and J. A. Gwinn, *J. Chem. Phys.*, 53, 2605 (1970).
(24) L. Mahan and M. Lapp, *Phys. Rev.*, 179, 19 (1969).
(25) R. G. Breene, Jr., *Acta Phys. Pol.*, A37, 477 (1970).
(26) R. S. Mulliken, *J. Chem. Phys.*, 55, 309 (1971).
(27) R. S. Mulliken, *ibid.*, 55, 288 (1971).
(28) G. S. Schwarzenback and K. Lutz, *Helv. Chim. Acta*, 23, 1139 (1940).

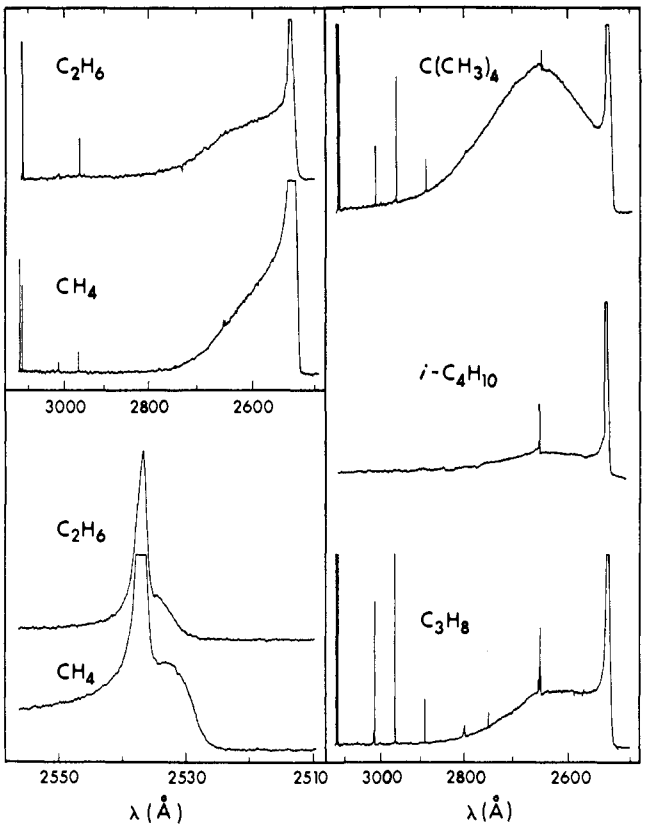

Figure 2. Microdensitometer trace of emission spectra. Lower left (2.16 OD): CH_4, 500 Torr, 1 hr; C_2H_6, 400 Torr, 15 min. Upper left: CH_4, 500 Torr, 1 hr (0.8 OD); C_2H_6, 600 Torr, 3 hr (0.8 OD). Right: C_3H_8, 600 Torr, 3 hr (0.8 OD); *i*-C_4H_{10}, 645 Torr, 15 min (0.4 OD); $C(CH_3)_4$, 510 Torr, 1.2 hr (0.8 OD).

Table II. Separation of Emission-Band Maxima in the c Region from the 2536.5 Å (39,424 cm^{-1}) Resonance Line

Compd	Press, Torr	$\Delta\omega$, cm^{-1}
NH_3	400	−11,330
H_2O	14	−4,880
C_2H_5OH	36	−6,150
CH_3OCH_3	235	−5,410
$C_2H_5OC_2H_5$	240	−5,810
Furan	180	−5,980
$C(CH_3)_3OC_2H_5$	88	−5,870

resonance line. The type "b" bands appear as a broadening, or a partially resolved shoulder, extending several hundred ångströms to the long wavelength side of the resonance line and the "c" type structureless bands are shifted toward still longer wavelengths and separated completely from the 2537-Å line. The intense sharp lines superimposed on the band spectra in Figures 1–6 originate from scattered light from the exciting mercury lamp.

The emission spectra observed in the presence of various noble gases around atmospheric pressure and at room temperature are displayed in Figure 1. With Ar and Xe, at least two, and with Kr, three type a bands appear. Asymmetrical broadening of the resonance line toward the short wavelength side in the presence of He and Ne indicates that these gases also give weak band fluorescence in this region. The a band positions in the case of Xe were independent of pressure between

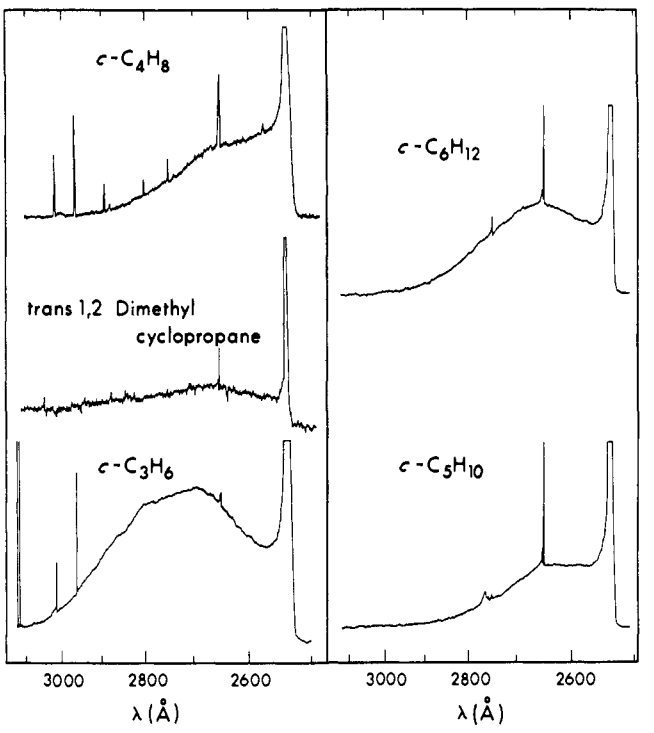

Figure 3. Microdensitometer trace of emission spectra. Left (0.4 OD): c-C_3H_6, 400 Torr, 1.5 hr; *trans*-1,2-dimethylcyclopropane, 80 Torr, 2 hr; c-C_4H_8, 720 Torr, 1.5 hr (0.8 OD). Right (0.4 OD): c-C_5H_{10}, 210 Torr, 55 min; c-C_6H_{12}, 70 Torr, 1 hr.

10 and 800 Torr whereas the b band maxima shifted to longer wavelengths with increasing pressure. This shift appears to result from a combination of the intensity profiles of the pressure-broadened resonance line and the band emission.

A consistent trend in the band positions can be observed throughout the noble gas series. Going from He to Xe, the maxima of the a bands shift toward the resonance line and become more intense. In addition, Ar, Kr, and Xe each give one type b band extending to 2600, 2700, and 3000 Å, respectively. Argon and krypton broaden the resonance line extensively towards longer wavelengths while xenon has a broad maximum at $\lambda \sim 2690 \pm 10$ Å. These spectra exhibit faint structures superimposed on the continuum near the resonance line while the xenon spectrum, in addition, displays weak structural features in the b band as well (marked with arrows in Figure 1).

A trend similar to that found with the noble gases is apparent in the spectra of the paraffins, Figure 2. A single short-wavelength band converges on the resonance line, while the b band shifts progressively to longer wavelengths as the molecular weight of the paraffin increases. Methane and ethane give only an asymmetrical broadening of the resonance line toward longer wavelengths but the larger molecules give a broad maximum beyond 2650 Å. Short wavelength bands were not observed with propane and the larger paraffins. Reducing the total pressure of neopentane to 8 Torr (see Table I) shifts the emission spectra slightly to shorter wavelengths. Cyclopropane, Figure 3, differs significantly from propane in that its b band extends to 3000 Å with a maximum at about 2690 Å. However, the spectra of the larger cycloparaffins are similar to the straight chain analogs.

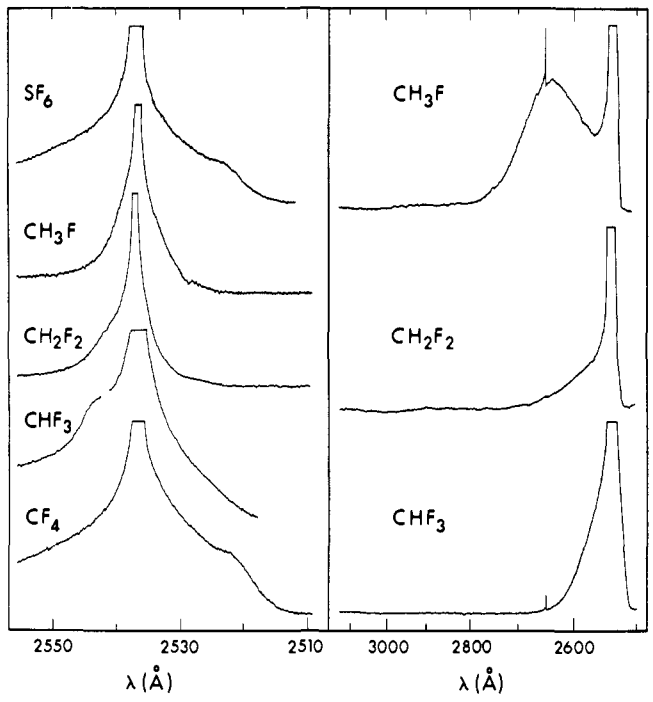

Figure 4. Microdensitometer trace of emission spectra. Left (2.16 OD): CF_4, 614 Torr, 30 min; CHF_3, 280 Torr, 15 min; CH_2F_2, 300 Torr, 15 min; CH_3F, 310 Torr, 15 min; SF_6, 190 Torr, 1 hr. Right (0.4 OD): CHF_3, 280 Torr, 15 min (0.8 OD); CH_2F_2, 310 Torr, 15 min; CH_3F, 330 Torr, 15 min.

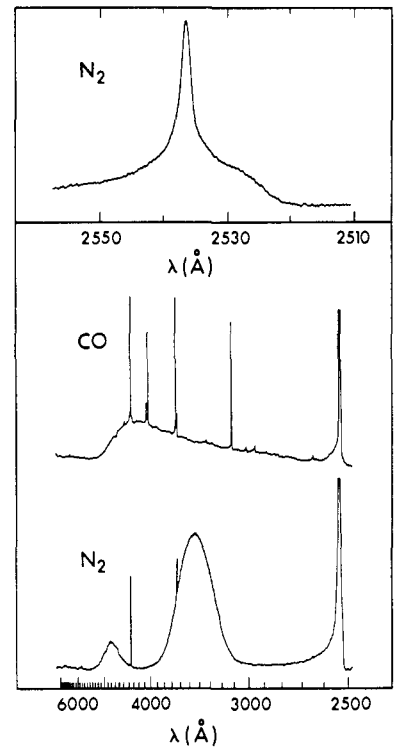

Figure 5. Microdensitometer trace of emission spectra. Below: N_2 700 Torr, 2.4 hr (0.8 OD); CO, 420 Torr, 4 hr (0.4 OD). Above: N_2, 600 Torr, 5.5 hr (2.16 OD).

The fluorescence spectra with SF_6 and the fluorinated methane series are shown in Figure 4. All spectra were obtained under identical conditions, at approximately 300 Torr of substrate pressure, and consequently their intensities should be directly comparable.

On progressive fluorine substitution in methane the following changes can be noted, Table I. (i) The a bands shift gradually to longer wavelength which in the case of CHF_3 results in the appearance of the a band on the long-wavelength side of the resonance line. On perfluorination however, the a band shows an abrupt short-wavelength shift. (ii) The b band with CH_3F shows a maximum at about 2630 Å extending to about 2740 Å, while CH_2F_2 gives a weaker band as an asymmetric broadening of the resonance line extending to about 2660 Å. The b band of CHF_3 is again more intense and extends to only about 2640 Å. It will also be noted that the spectrum of SF_6 is nearly identical with that of CF_4.

Figure 5 displays the fluorescence spectra obtained with nitrogen and carbon monoxide. The 3420- and 4820-Å bands attributed to the $A(^3l_u)$ and $A(^3O_u^-)$ states of the diatomic mercury excimer[29] appear intensely in the nitrogen spectrum. The b band of nitrogen is seen as a broadening of the resonance line on the long-wavelength side and the a band as a hump on the short-wavelength side.

The carbon monoxide spectrum is somewhat different in that it is extremely weak and broad; its intensity increases gradually to the limit of the plate sensitivity at 5000 Å.

The fluorescence spectra in the presence of ammonia, water, alcohol, and various ethers are shown in Figure 6. Each of these exhibits a structureless c-type band,

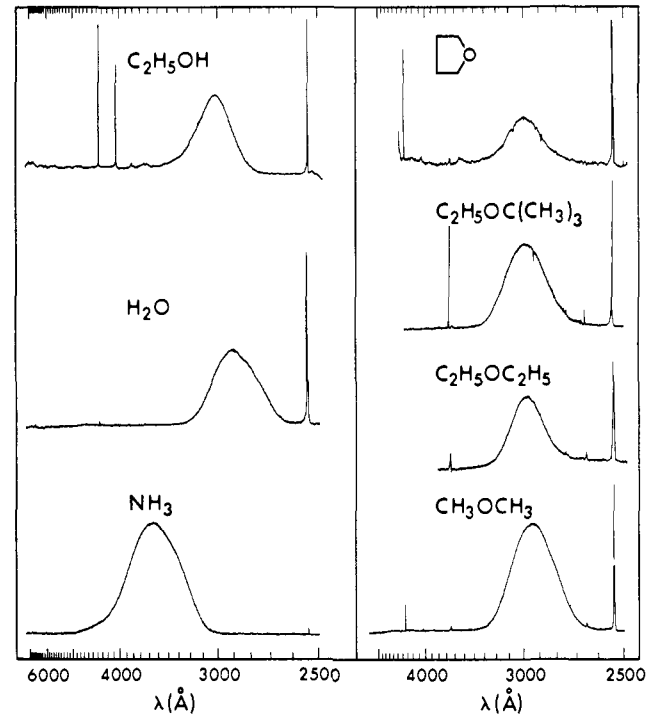

Figure 6. Microdensitometer trace of emission spectra. Left (2.16 OD): NH_3, 400 Torr, 1 min; H_2O, 14 Torr, 15 min; C_2H_5OH, 36 Torr, 16 min (0.4 OD). Right: CH_3OCH_3, 235 Torr, 1 hr (2.16 OD); $C_2H_5OC_2H_5$, 240 Torr, 145 min (0.8 OD); $C_2H_5OC(CH_3)_3$, 88 Torr, 5 hr (2.16 OD); tetrahydrofuran, 108 Torr, 3 hr (0.4 OD).

completely detached from the resonance line. The emission intensities vary markedly in the order NH_3 > H_2O > $(CH_3)_2O$ > C_2H_5OH > $C_2H_5OC(CH_3)_3$ >

(29) S. Mrozowski, *Rev. Mod. Phys.*, **16**, 153 (1944).

Table III. Physical Properties of Reagents

Compd	Hg* quenching cross section,[a] Å²	Dipole moment,[b] $\mu \times 10^{18}$ esu	Polarizability α,[c] Å³	IP,[b] eV	L-J force constants[d] σ, Å	ϵ/k, °K
He	0.20[e]	0	0.206[f]	24.48	2.556[l]	10.22
Ne	0.27[e]	0	0.398[f]	21.56	2.749[l]	35.6
Ar	0.32[e]	0	1.63[f]	15.75	3.405[l]	119.8
Kr	0.34[e]	0	2.84[f]	14.00	3.60[l]	171.0
Xe	0.12[e]	0	4.01[f]	12.13	4.10[l]	221.0
CH_4	0.091	0	2.60	12.60	3.758	148.6
C_2H_6	0.22	0	4.47	11.50	4.443	215.7
C_3H_8	3.1	0.08	6.29	11.10	5.118	237.1
i-C_4H_{10}	7.5	0.132	8.14	10.57	5.278	330.1
$C(CH_3)_4$	2.2	0		10.35	6.464	193.4
c-C_3H_6	2.0	0		10.09	4.807	248.9
c-C_6H_{12}	23.0		10.80	9.80		
CH_3F	$\sim 2 \times 10^5$ [i]	1.85	2.61[g]	12.85	3.73	333.0
CH_2F_2		1.97	2.73[g]	10.30	4.08	318.0
CHF_3	0.007	1.65	2.80[g]		4.33	240.0
CF_4	v small	0	2.85[g]	17.8[i]	4.662	134.0
SF_6		0		19.3[k]	5.128	222.1
Hg ($^1S_0$)		0	5.17[f]	10.43	2.898[l]	851.0
NH_3	4.5	1.30	2.26	10.20	2.900	558.3
H_2O	1.5	1.87	5.16	12.60	2.641	809.1
C_2H_5OH	34.0	1.69	8.37	10.49	4.530	362.6
$(CH_3)_2O$	19	1.30		9.98	4.307	395.0
$(C_2H_5)_2O$	52	1.15		9.60	5.678	313.8
Furan		1.63		9.45[k]		
Hg ($^3P_1$)			20.0[h]	5.63		

[a] To be published. [b] "Handbook of Chemistry and Physics," 50th ed, Chemical Rubber Publishing Co., Cleveland, Ohio, 1969. [c] H. H. Landolt and R. Bornstein, "Zahlenwerte und Functionen aus Physik, Chemie, Astronomie, Geophysik und Technik," Band I, Teil 3, Springer-Verlag, Berlin, 1950, pp 511–512. [d] R. A. Svehla, NASA Technical Report, R 132 (1962). [e] Reference 8. [f] Footnote *c*, Band I, Teil 1, p 401. [g] A. D. Buckingham and B. J. Orr, *Trans. Faraday Soc.*, **65**, 673 (1969). [h] Reference 1, p 178. [i] Footnote *c*, p 367. [j] J. D. Allen and M. C. Flowers, *Trans. Faraday Soc.*, **64**, 3300 (1968). [k] V. I. Vedeneyev, L. V. Gurich, V. N. Kondrat'yev, V. A. Medveder, and Y. L. Frankevich, "Bond Energies, Ionization Potentials and Electron Affinities," St. Martins Press, New York, N. Y., 1966. [l] Reference 31, p 1110.

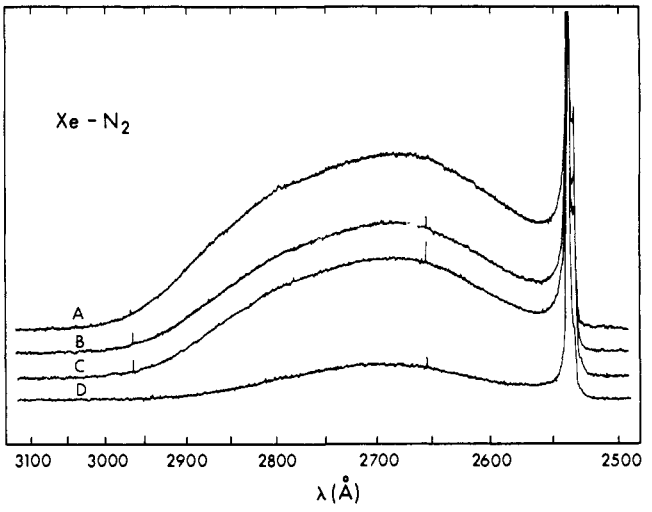

Figure 7. Microdensitometer trace of emission spectra from Xe–N_2 mixtures, 5-min exposure time, total pressure = 199 Torr: (A) 100% Xe, (B) 73% Xe, (C) 55% Xe, (D) 30% Xe.

$(C_2H_5)_2O$ ~ tetrahydrofuran. Increasing the size of the ether groups also causes an increase in the separation of the band maxima from the resonance line, Table II.

In order to ascertain whether the emission originates from the complex formed from Hg ($^3P_1$) + substrate or Hg ($^3P_0$) + substrate, band-fluorescence spectra were recorded from the sensitization of propane and xenon in the presence of varying concentrations of nitrogen. Keeping the total pressure at 200 Torr, a variation of propane concentration from 100 to 11% reduced the emission intensity only by about 20% at $\lambda \sim 2620$ Å. Figure 7 displays the spectra obtained from various Xe–N_2 mixtures and shows that as the nitrogen percentage is increased in the mixture, the band fluorescence intensity decreases.

Lennard-Jones Force Constants. The empirical Lennard-Jones[30] (6–12) potential function has been extensively used to describe the interaction of two

$$V(r) = 4\epsilon\left[\left(\frac{\sigma}{r}\right)^{12} - \left(\frac{\sigma}{r}\right)^{6}\right] - C_{12}r^{-12} - C_6r^{-6}$$

spherically symmetric colliding species. The quantity σ is the finite internuclear distance where the potential function is zero and ϵ is the depth of the potential well. The Lennard-Jones force constants for the interaction of ground-state mercury with various substrates have been computed employing the mixture rules $\epsilon_{mix} = (\epsilon_1 \times \epsilon_2)^{1/2}$ and $\sigma_{mix} = (\sigma_1 + \sigma_2)/2$.

To calculate ϵ for the collision of Hg* with different molecules, London's relationship[31] for the attractive part of the potential was employed (eq I) where α_1

$$V(r) \simeq -\frac{3}{3}\frac{\alpha_1\alpha_2}{r^6}\frac{I_2I_2}{(I_1 + I_2)} \qquad (I)$$

and α_2 are the polarizabilities and I_1 and I_2 are the ionization potentials of the colliding species. A correction factor was established for each collision pair by computing C_6 for the ground-state mercury interaction

(30) J. E. Lennard-Jones, *Proc. Roy. Soc., Ser. A*, **106**, 463 (1924).
(31) J. O. Hirschfelder, C. F. Curtiss, and R. B. Bird, "Molecular Theory of Gases and Liquids," Wiley, New York, N. Y., 1954, p 963.

Table IV. Lennard-Jones Force Constants for the Collision of Ground- and Excited-State Mercury with Different Atoms and Molecules

Collision partner	Hg ($^1S_0$)		Hg ($^3P_1$)			
	ϵ, kcal mol^{-1}	σ, Å	C_6^*, $\times 10^{-11}$ erg Å^6	ϵ^*, kcal mol^{-1}	σ^*, Å	$\sigma - \sigma^*$, Å
Ar	0.634	3.152	12.51	1.28	3.30	−0.15
Kr	0.757	3.249	18.13	1.74	3.34	−0.09
Xe	0.861	3.499	27.44	2.29	3.52	−0.02
				(4.47)	(3.15)	+0.35
CH_4	0.706	3.328	18.40	1.76	3.38	−0.05
C_2H_6	0.851	3.671	30.28	2.28	3.69	−0.02
C_3H_8	0.892	4.008	41.65	3.89	3.72	+0.29
i-C_4H_{10}	1.052	4.088	52.93	4.30	3.84	+0.25
$C(CH_3)_4$	0.805	4.681	63.16	4.12	4.24	+0.44
CH_3F	1.057	3.314	18.52	4.49	3.08	+0.23
CHF_3	0.897	3.614	20.40	2.18	3.68	−0.07
CF_4	0.671	3.780	22.97	1.08	4.10	−0.32
SF_6	0.863	4.013	37.34	1.71	4.21	−0.20
Hg ($^3P_1$)	1.689	2.898	32.59	14.76	2.40	+0.498

by eq I and then comparing it with the value calculated using ϵ_{mix} and σ_{mix}. The computed values of C_6^* obtained from expression I for the interaction of Hg* with different species were multiplied by this factor. Input parameter values employed in the calculations are listed in Table III together with some other physical properties of the reagents. The results of these computations are compiled in Table IV.

Discussion

The shape and intensity of fluorescence bands are determined by the exact position and shape of the upper and lower potential surfaces, the vibrational and rotational energy of the upper state, and the oscillator strength of the transition. Herzberg[32] discussed the effect of the shape of potential surfaces on the emission spectra of diatomic molecules and showed that continuous spectra are expected on both the long- and short-wavelength sides of the resonance line when weakly bonding van der Waals molecules are present. In general, fluorescence bands observed in the mercury photosensitization of noble gases, paraffins, fluoromethane, and SF_6 fall into this category.

The a bands of Ar, Kr, and Xe are similar to those observed by Oldenberg[3] with the exception that Kr gives three bands rather than two as reported by Oldenberg. This, however, is in agreement with the spectrum obtained in absorption at high densities[17] where the same three bands appeared distinctly. The band positions in the xenon spectrum are not affected by pressure between 10 and 800 Torr of Xe suggesting that multiple interactions of mercury with more than one gas atom do not contribute to the intensity of these fluorescence bands.

The structural features superimposed on the red-shifted b bands of Ar, Kr, and Xe are significant because they are indicative of transitions between discrete levels, most likely quantized vibrational levels of the upper and lower states of the van der Waals molecules.

Contrary to the assignment of Freeman, *et al.*,[15] we attribute the b bands of the noble gases to the transitions of the Hg ($^3P_1$) instead of the Hg ($^3P_0$) atom complexes. This assignment is based on the following experimental information: (a) the xenon spectrum extends smoothly on the short-wavelength side to the 2537-Å resonance line; (b) the b bands with Ar and Kr are both blue shifted as compared to the 2654-Å line of the Hg ($^3P_0$) atom; (c) lowering of the partial pressure of xenon in the Xe + Hg + N_2 system results in a decline of the emission intensity; and (d) attempts to detect Hg ($^3P_0$) atoms in the noble gas systems were all unsuccessful.

The existence of a- and b-type bands in the spectra of paraffins shows that complex formation between the excited mercury atom and the paraffin molecule is a general feature of these systems. The dissociative lifetimes of these complexes are short, and can be estimated from the pressure dependence of the b band maximum in the neopentane system to lie in the order of 10^{-9} sec.

The band fluorescence spectra associated with the mercury resonance line in the presence of the rare gases and paraffins are quite similar and can be compared with the absorption spectra of the alkali metals Na, Rb, and Cs in the presence of these reagents.[16] In the case of alkali metals, the violet bands appear several hundred wavenumbers from the resonance line, while the red bands are shifted only some 20 to 90 cm^{-1} away. The red band maxima are separated from the spectral line only for the heavier gases, such as xenon, krypton, and saturated hydrocarbons containing more than three carbon atoms. The shifts in the spectra with molecular weight and polarizability are believed to be related to changes in the van der Waals interactions in both the ground and excited states. Except for the absolute magnitudes of the band positions, the trends observed in the mercury systems are similar to these, and appear to correlate with the mean polarizability of the paraffin (Table III).

A significant difference between the alkali metal–paraffin and mercury–paraffin systems is the occurrence of sensitized decomposition in the latter and its absence in the former. The decomposition is thought to take place *via* a predissociation type process which would affect primarily the shape and intensity of the a bands. Emission and predissociation are competing processes and the most intense spectra are obtained in systems like CH_4, C_2H_6, and neopentane, where the decomposition quantum yields are considerably lower than unity.[33]

The spectrum of cyclopropane which, although in shape and intensity is similar to the rest of the paraffin

(32) G. Herzberg, "Molecular Spectra and Diatomic Structure, I. Spectra of Diatomic Molecules," Van Nostrand, Princeton, N. J., 1950, pp 377–400.

(33) J. G. Calvert and J. N. Pitts, "Photochemistry," Wiley, New York, N. Y., 1966, Chapter 2.

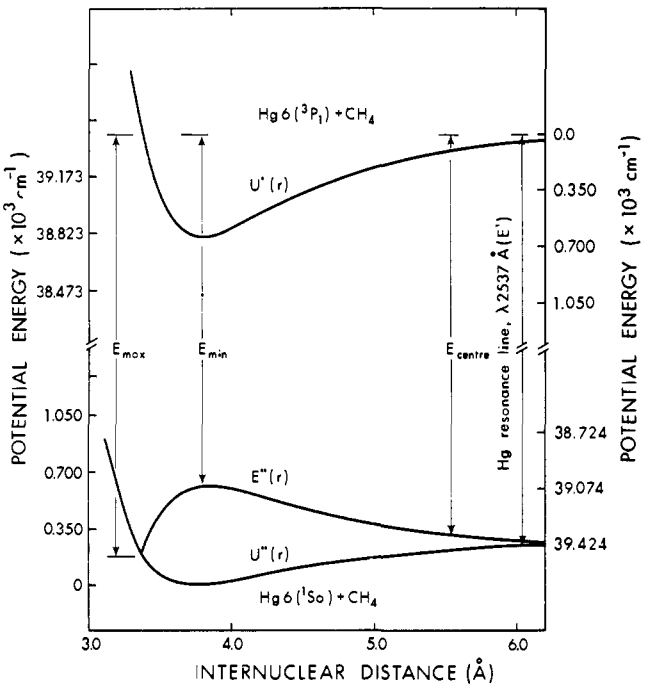

Figure 8. Potential curves for mercury–methane interaction.

spectra, may be due to a complex of the structure, [Hg*·Δ], rather than the [Hg*·HR] structure of the other paraffins because in cyclopropane the major mode of decomposition is C–C bond cleavage[34,35] whereas with all other paraffins only C–H bond cleavage occurs.

It is also significant that the b bands of paraffins extend on the short-wavelength side to the mercury resonance line, from which we conclude that the bands are primarily due to Hg ($^3P_1$) rather than Hg ($^3P_0$) complexes.

The band fluorescence spectra in the presence of fluorinated methanes are more difficult to correlate with physical parameters. For compounds with no permanent dipole moment, the shift of the a band from the resonance line does not appear to be related to the mean polarizability. The fact that the band spectra from the partially fluorinated methanes differ markedly from those of CH_4, CF_4, and SF_6 is related to the presence of a permanent dipole.

Nitrogen and carbon monoxide quench Hg ($^3P_1$) atoms mainly *via* spin–orbit relaxation to the $^3P_0$ state. The metastable atoms react with ground-state mercury atoms in the presence of nitrogen to give Hg_2 (^3l_u) which is responsible for the band around 3420 Å. The (^3l_u) molecules convert to the (^3O_u) state in a pressure-induced transition[36–38] and emission from the latter state results in the appearance of the band around 4820 Å. The weak a and b bands of N_2 are seen as broadening on the respective side of the mercury resonance line.

The b band of CO has a unique shape and is the farthest removed from the mercury resonance line yet found. This seems to manifest the exceptional stability of the mercury carbonyl structure [·Hg←|C≡O:] proposed by Polanyi, *et al.*[39,40]

The single, structureless c-type bands in the spectra of NH_3, H_2O, and C_2H_5OH also reported by Freeman, *et al.*, are due to complexes in which the excited mercury atom is bound to the nonbonding p orbital of the heteroatom [·Hg←|NH_3] and [·Hg←|ORH]. The separation of band maxima, Table II, could be correlated with the electron donating ability of the substrate if steric interference is invoked. This trend is in agreement with the earlier postulate regarding the electrophilic nature of the excited mercury atom and the variation in quenching ability with the nucleophilicity of quencher.[41]

The emission yields are particularly high with NH_3 and H_2O and gradually decline as the complexity of the molecule increases. This is in line with the high bond energies and the consequent inefficiency of the competing chemical processes in NH_3 and H_2O.

The molecules producing c-type bands are all known to yield Hg ($^3P_0$) atoms by spin–orbit relaxation and the complexing is presumably with the metastable atoms.

In the application of the Franck–Condon principle to fluorescence processes from high vibrational levels of excited states, it has customarily been assumed that transitions occur at internuclear distances corresponding to the classical turning points because of the high probability of this configuration. As mentioned before, Mulliken[26] has recently shown that the turning points are not the only positions giving maximum probability of transition. For the simplified situation where the upper potential surface is represented by a parabola and the lower surface by a bonding curve, a second maximum in the transition probability, from a high vibrational level of the upper surface, may occur in the neighborhood of the equilibrium configuration where the kinetic energy is maximum.

The observed a- and b-type satellite bands can be described in terms of Mulliken's theory. Accordingly the excited mercury atom and reactant molecule combine along a slightly attractive potential surface with a shallow well to form a complex which may possess quantized vibrational-rotational levels.[18,20] For the illustration of the origin of band spectra, computed Lennard-Jones potential curves for the interaction of ground- and excited-state mercury with methane are displayed in Figure 8. If $U'(r)$ and $U''(r)$ represent the potential energy variation as a function of the internuclear distance in the upper and lower state, then the spectral distribution of fluorescence is given by $E''(r) = E' - U'(r) + U''(r)$, where E' is the energy of the resonance line. Following Mulliken, the classical treatment yields a smooth continuum of frequencies between ν_{center} and ν_{min} as well as between ν_{min} and ν_{max}. But the quantum mechanical Franck–Condon overlap integral can yield either a continuum or a banded structure, depending upon whether the potential curves are quantized or not. If the location of the up-

(34) D. W. Setser, B. S. Rabinovitch, and E. G. Spittler, *J. Chem. Phys.*, 35, 1840 (1961).
(35) O. P. Strausz, P. J. Kozak, G. N. C. Woodall, A. G. Sherwood, and H. E. Gunning, *Can. J. Chem.*, 46, 1317 (1968).
(36) S. Penzes, H. E. Gunning, and O. P. Strausz, *J. Chem. Phys.*, 47, 4869 (1967).
(37) J. E. McAlduff, D. D. Drysdale, and D. J. LeRoy, *Can. J. Chem.*, 46, 199 (1968).
(38) S. Penzes, H. S. Sandhu, and O. P. Strausz, *Int. J. Chem. Kinet.*, 4, 449 (1972).
(39) G. Karl, P. Kruus, and J. C. Polanyi, *J. Chem. Phys.*, 46, 224 (1967).
(40) G. Karl, P. Kruus, J. C. Polanyi, and U. M. Smith, *ibid.*, 46, 244 (1967).
(41) H. E. Gunning and O. P. Strausz, *Advan. Photochem.*, 1, 209 1963.

per potential curve is such that the left-hand turning point is right above or near the internuclear equilibrium distance of the lower curve, the short-wavelength satellite bands will appear. Formation of more than one satellite band on the short-wavelength side of the resonance line is due to transitions to various vibrational states of the lower curve. In the calculation of $U'(r)$ it is assumed that the band maxima on the long-wavelength side of the resonance line correspond to a maximum probability of emission near the bottom of the upper potential well. From the calculated value of C_6^* a best fit to the experimental separation of the emission-band maxima was obtained by varying σ^*. The results for systems which give band maxima in the a and/or b regions are listed in Table IV and a comparison of calculated and observed band maxima positions is presented in Table V.

Table V. Comparison of Observed Separations of Band Maxima from the Resonance Line with Those Computed from Lennard-Jones Force Contants Given in Table IV

Collision partner	$\Delta\omega$, cm^{-1} Obsd	Calcd Blue	Calcd Red
Ar	164	162	−245
Kr	128	137	−352
Xe	58	43	−502
	~−2000		−1994
CH_4	65	80	−371
C_2H_6	29	26	−502
C_3H_8	−1260		−1275
i-C_4H_{10}	−1260		−1293
$C(CH_3)_4$	−1830		−1700
CH_3F	−1500		−1461
CHF_3	−97	110	−454
CF_4	220	222	−189
SF_6	220	219	−319

In the case of the Hg + Xe system two sets of L-J force constants are required to reproduce the a and b band maxima. In this connection it should be noted that the $^3P_1$ level of the mercury atom may split into three nondegenerate states with $m_J = -1, 0, 1$ in the presence of an external perturber giving rise to three different electronic states in the (Hg·substrate)* complex. In the case where the perturber is an atom the +1 and −1 states are degenerate and two states with $\Omega = 0$ and $\Omega = \pm 1$ result. It is possible that one of the bands in the Hg* + Xe system originates from one state and the other from the other state. In the rest of the computations the entire spectrum was assumed to originate from a single upper state of the complex.

It is interesting to note how the equilibrium internuclear distance varies in the paraffin series with molecular size and polarizability. In going from methane to neopentane the excited-state equilibrium internuclear distance (which is proportional to σ) decreases as compared to the equilibrium distance of the ground-state molecule, and in neopentane the equilibrium distance of the excited state is about 0.5 Å shorter than that of the ground state. This phenomenon may have consequences with regard to the mechanism of the energy transfer reaction in that it could lead to radiationless transitions *via* curve crossing, especially from the Hg ($^3P_0$)·substrate surface. This intersystem crossing with the conversion of electronic energy into translational and vibrational modes could explain the low quantum efficiency of the Hg ($^3P_0$) atom sensitized decomposition of paraffins.[42]

Band emission was also looked for but not detected in the Hg ($^3P_1$) sensitization of the following substrates: C_2H_4, C_2H_3F, C_2F_4, $C_2H_2F_2$, C_3H_6, O_2, H_2, NO, N_2O, CO_2, CH_3CHO, $CH_3OCH{=}CH_2$, thiophene, NO_2, SiD_4, $(CH_3)_2SiH_2$, furan, and benzene. With benzene and C_6F_6, owing to excitation by direct absorption, the fluorescence spectrum appeared weakly.

Acknowledgment. We thank the National Research Council of Canada for financial assistance, Dr. E. M. Lown for reading the manuscript, and Mr. A. Clement for assistance in the experimental work.

(42) J. M. Campbell, O. P. Strausz, and H. E. Gunning, *J. Amer. Chem. Soc.*, 95, 740 (1973).